Available online at www.sciencedirect.com
ScienceDirect
Trans. Nonferrous Met. Soc. China 33(2023) 3017−3026
Transactions of Nonferrous Metals Society of China
www.tnmsc.cn

Environment-dependent phase stabilities of titanium hydrides: First-principles prediction

Chun-lei SHEN[1], Yi LIU[2], Yu-xiang GONG[2], Zheng-qing LIU[2], Yong JIANG[2,3], Can-hui XU[1], Xiao-song ZHOU[1], Xing-gui LONG[1]

1. Institute of Nuclear Physics and Chemistry, China Academy of Engineering Physics, Mianyang 621900, China;
2. School of Materials Science and Engineering, Central South University, Changsha 410083, China;
3. State Key Laboratory of Powder Metallurgy, Central South University, Changsha 410083, China

Received 9 April 2022; accepted 30 August 2022

Abstract: Various phases of TiH_x (x=1−2) were constructed, with all possible H-atom configurations being considered. The first-principles energetics calculations were performed to evaluate their formation preference and mechanical and thermodynamic stabilities. All the results were then combined to construct the stable and metastable phase stability diagrams of TiH_x. It is suggested that many stable and metastable TiH_x phases have very comparable formation energies and thus are likely to co-exist. Their relative stabilities are strongly depended on temperature (T) and the partial pressure of hydrogen ($p(H_2)$). Over the entire T and $p(H_2)$ range of interest, γ-TiH and γ-TiH_2 are the only two stable phases. ε-TiH, γ-$TiH_{1.5}$, ε- and δ-$TiH_{1.75}$, and ε-TiH_2 can possibly present as metastable phases. These metastable phases are all mechanically stable, and have a thermodynamic tendency to continuously absorb or release H until reaching the equilibrium phases of γ-TiH_2 or γ-TiH.

Key words: titanium hydride; phase stability; metastable phase; first-principles

1 Introduction

Titanium hydrides have been found many promising applications for solid state hydrogen storage and absorption of nuclear radiation in thermonuclear energy production [1−3]. The Ti−H equilibrium system is essentially a simple eutectoid system, with the terminal constituents being a hexagonal close-packed (hcp) α-Ti solution and a hydride phase of TiH_x (x=1−2) [4,5]. Hydrogen has great influence on titanium phase stability. The high temperature body-centered cubic β-Ti phase can be stabilized by dissolved hydrogen to a temperature almost 600 °C below the $\alpha \rightleftharpoons \beta$ transition temperature. At the high hydrogen content end (50−60 at.%) of the eutectoid reaction, titanium hydrides TiH_x (x=1−2) may possess various different structures, including the face-centered cubic phase fcc-δ, and two face-centered-tetragonal phases fct-γ (c/a>1) and fct-ε (c/a<1) [6−14]. Phase transitions among δ, γ, and ε can be triggered by tuning the temperature (T) and/or the partial pressure of hydrogen ($p(H_2)$), both determining the equilibrium hydrogen contents of TiH_x (x=1−2).

Many uncertainties of titanium hydrides still remain concerning their atomic structures and relative stabilities, perhaps largely due to the extreme difficulties in experimentally determining the amount of hydrogen atoms and their occupation sites in hydrides. One major concern is about the relative stabilities of fct-γ and fct-ε with respect to fcc-δ during the hydrogenation process of titanium and the service period of titanium hydrides. For

Corresponding author: Yong JIANG, Tel/Fax: +86-731-88836320, E-mail: yjiang@csu.edu.cn;
Xing-gui LONG, Tel/Fax: +86-816-2489387, E-mail: xingguilong@caep.cn
DOI: 10.1016/S1003-6326(23)66314-9
1003-6326/© 2023 The Nonferrous Metals Society of China. Published by Elsevier Ltd & Science Press

instance, some Ti−H phase diagrams [15] showed the existence of γ as a stable phase and some did not [4,16]. OKAMOTO [17] suggested the hydrogen content of γ phase to be 58.5%−66.7%, corresponding to a composition range of $TiH_{1.4-2}$. NUMAKURA and KOIWA [18], however, suggested that similarly as in zirconium hydrides, δ, γ, and ε phases could be all formed in titanium hydrides. All these experimental studies must be viewed with some cautions, since there is doubt as to the purity of the titanium, and furthermore, the oxide layers of impurities on titanium surfaces may affect the equilibrium absorption of hydrogen.

To address the experimental challenges, a number of first-principles calculations have been devoted to exploring the formation energies and atomic structures of titanium hydrides, to assess their relative stabilities and predict the phase transitions of $\varepsilon \rightleftharpoons \delta$ and $\gamma \rightleftharpoons \delta$ [19−24]. Some broad findings have been achieved. Both γ-TiH and γ-$TiH_{1.25}$ can be stable. $TiH_{1.5}$ tends to present as γ, but other phases have fairly comparable formation energies. $TiH_{1.75}$ and TiH_2 can form ε and δ phases with only a small energy difference between each other. Nevertheless, some disputes arose among these theoretical studies. For instance, γ-TiH was predicted to be stable according to a density functional theory (DFT) study [21] but instable with a tendency to decompose into hcp Ti and δ-TiH_2 according to another DFT study [19]. Experiments cannot help solve such disputes. Various experimental studies have demonstrated that γ-TiH can be metastable only [4], but in DING and JONES phase diagram [25], γ-TiH exists as a stable phase at low temperatures.

In this study, first-principles calculations were employed to revisit the atomic structures and the relevant energetics of various possible phase structures (δ, γ, and ε) of TiH_x (x=1−2) with the H concentration range of 50%−66.7%. The formation energetics, mechanical and thermal stabilities of TiH_x were thoroughly investigated and compared. Finally, all the results were combined to construct the stable and metastable phase stability diagrams of Ti−H system with respect to the environmental conditions of T and $p(H_2)$.

2 Computational methods

All the first-principles calculations were performed using density functional theory (DFT) code, Vienna Ab-initio Simulation Package (VASP) with the plane-wave basis sets and periodic boundary conditions [26]. The plane−wave basis sets were generated with valence configurations of Ti-$3s^2 3p^6 3d^2 4s^2$ and H-$1s^1$. The electron−ion interactions were described by the projector augmented wave (PAW) method within the frozen-core approximation [27,28]. The exchange−correlation functionals were treated within the generalized gradient approximation (GGA) of Perdew−Burke−Ernzerhof (PBE) [29]. The convergence tests were conducted with respect to the kinetic energy cutoff of the plane−wave basis and the k-mesh size for Brillouin-zone integration. The self-consistence convergence criterion for electron iterations was set to be 10^{-5} eV/atom, and the ground-state atomic geometries were optimized by minimizing the Hellman–Feynman force until the total force on each ion was converged to be 0.01 eV/Å. A high energy cutoff of 480 eV and a 7×7×7 Monkhorst−Pack k-mesh proved sufficient for bulk calculations. The structural relaxation calculations were performed over all possible configurations of H atoms under a constraint of the total number of H atoms (from four to eight). During the relaxation, all the ion positions and the cell volume were allowed for full relaxation, while the cell shape remained unchanged.

3 Results and discussion

3.1 Bulk structures and formation energies of TiH_x

Neutron inelastic scattering measurement showed that hydrogen occupies the tetrahedral-interstitial site in titanium hydrides [30]. To calculate an fcc or fct structure of TiH_x, the 4-atom conventional unit cell of fcc-Ti was always adopted as the starting structure in Fig. 1. All possible tetrahedral-interstitial sites are purposely labeled as a−h. A total number of 4, 5, 6, 7 or 8 H atoms are assigned to these sites, to construct the TiH_x supercell with a composition of x=1, 1.25, 1.5, 1.75 or 2, respectively. For instance, the [-*adeh*-] structure of TiH indicates that four H atoms occupy the interstitial sites of a, d, e, and h. We first predicted the total energy versus volume data for various TiH_x (x=1, 1.25, 1.5, 1.75, 2). The results were fitted into the Murnaghan's equation of state

for solving lattice constants. For each composition, all possible configurations of H atoms have been considered, and further for each H-atom configuration, the c/a ratio varied from 0.80 to 1.20 with an interval of 0.02, to search for the minimal energy structure through full relaxation calculations.

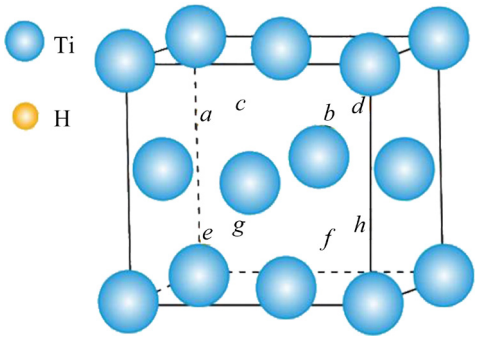

Fig. 1 Potential interstitial sites for H in bulk TiH_x (x=1−2)

The formation energy of TiH_x per conventional unit cell can be approximated as

$$\Delta E_f(TiH_x) = \mu^0_{TiH_x} - \mu^0_{Ti} - \frac{x}{2}\mu^0_{H_2} \quad (1)$$

where μ_i^0 is the unit energy or chemical potential of i (i=TiH_x, α-Ti, or H_2 molecule) at its standard state. A negative ΔE_f value indicates an energy-favored formation. Note that all these potential terms are temperature and pressure dependent, especially for H_2 molecules. But nevertheless, to evaluate the relative formation preference among different H-atom configurations under a given H content of TiH_x, all these energy terms can be calculated at their ground states (0 K) as the first order of approximation.

Table 1 summarizes the calculated formation energies and lattice constants for TiH_x with all possible H-atom configurations after full relaxation. The structure type of TiH_x can be determined by the optimized lattice constants. The initial arrangements of interstitial H atoms may break the fcc symmetry. Also, it has been widely reported in the literatures that different hydride phases may exist with the same H content. Thus, to consider all potential stable or metastable phases, we stretched or compressed very slightly the c axis to impose an initial fct type (γ or ε) distortion for each given H content prior to relaxation. It is clear from Table 1 that all these H-atom configurations in TiH_x were predicted with a negative formation energy and thus can be suggested as energetically feasible. Relaxation calculations of TiH, $TiH_{1.25}$, and $TiH_{1.5}$ converged into multiple local-minima that correspond to a total of ten, five, and five types of H-atom configurations in Table 1, respectively. Some local-minima have the same or very comparable formation energy values, suggesting that one or more metastable hydride structures might exist under a given H content. In particular, two lowest-energy structures can be suggested for TiH, $TiH_{1.25}$, and $TiH_{1.5}$, one being fct-γ (c/a>1) and the other being orthorhombic ($a\neq b\neq c$) with the same formation energy. The orthorhombic TiH_x has been never experimentally reported and can thus be tentatively discarded. All the predicted fct-γ results are compared favorably with available experiments and/or calculations in the literatures. The lowest energy structure of γ-TiH was predicted to be [*adeh*]-TiH with a=b=4.179 Å, c=4.589 Å and c/a=1.10, in a good agreement with the experimental values of a=b=4.21 Å and c=4.59 Å and c/a=1.09 [18]. The lowest energy structure of γ-$TiH_{1.25}$ was predicted to be [*bcdfg*]-$TiH_{1.25}$ with a=b=4.250 Å, c=4.544 Å and c/a=1.07, in a good agreement with another calculation of a=b=4.226 Å, c=4.564 Å and c/a=1.08 [22]. The lattice constant discrepancies are generally within 1%. For $TiH_{x>1.25}$, various H-atom configurations with similar lattice constants may co-exist, due to their very comparable formation energies. For instance, γ-$TiH_{1.5}$ may have a=b=4.323−4.363 Å, c=4.412−4.498 Å and c/a=1.01−1.04, all of which have a very small energy difference of 0.03 eV/cell only. For $TiH_{1.75}$, γ is predicted as the lowest energy phase, but δ, and ε phases sharing the same H-atom configuration are almost equally preferred in energy. Thus, the three phases are very likely to co-exist. For the same reason, it can be also predicted that the γ and ε phases of TiH_2 may co-exist. γ or ε-TiH_2 has been previously suggested by different DFT calculations [22,24] and also identified as the stable phase in different experiments [1,4].

3.2 Mechanical stabilities of TiH_x

Elastic constants C_{ij} determine how a crystal responds to external stresses in the elastic regime, and thus are often employed for assessing the mechanical stabilities of crystal subject to elastic distortion [31]. According to Nye's proposal [32],

Table 1 Predicted lattice constants, formation energies and structure types for TiH_x with different H-atom configurations

Hydride	H-atom configuration	ΔE_f/(eV·cell^{-1})	a/Å	b/Å	c/Å	c/a	Predicted phase
TiH	*adeh*	−2.952	4.179	4.179	4.589	1.10	γ
	cdef	−2.952	4.147	4.582	4.215	1.02	−
	defg	−2.696	4.433	4.433	4.096	0.92	ε
	abfg	−2.696	4.105	4.423	4.431	1.08	−
	aefh	−2.68	4.422	4.098	4.425	1.01	−
	cdfh	−2.672	4.423	4.423	4.090	0.93	ε
	bceh	−2.536	4.730	4.730	3.512	0.74	ε
	efgh	−2.432	4.197	4.197	4.538	1.08	γ
	cdgh	−2.432	4.530	4.141	4.263	0.94	−
	abce	−2.352	4.255	4.255	4.469	1.05	γ
	Expt. [18]		4.21	4.21	4.59	1.09	γ
	Calc. [22]		4.171	4.171	4.587	1.10	γ
	Calc. [19]		4.168	4.168	4.584	1.10	γ
$TiH_{1.25}$	*bcdfg*	−3.582	4.250	4.250	4.544	1.07	γ
	bdefg	−3.582	4.550	4.129	4.361	0.96	−
	defgh	−3.375	4.301	4.301	4.443	1.03	γ
	bdefh	−3.375	4.311	4.439	4.297	0.99	−
	adefg	−3.366	4.343	4.343	4.401	1.01	γ
	Calc. [22]		4.226	4.226	4.564	1.08	γ
$TiH_{1.5}$	*bcdfgh*	−4.340	4.356	4.356	4.407	1.01	γ
	abcdef	−4.340	4.352	4.400	4.367	1.01	−
	bcefgh	−4.320	4.363	4.363	4.412	1.01	γ
	abcefh	−4.320	4.414	4.356	4.366	0.99	−
	acdefh	−4.310	4.323	4.323	4.498	1.04	γ
	Calc. [22]		4.355	4.355	4.394	1.01	γ
	Calc. [23]		4.360	4.360	4.404	1.01	γ
	Calc. [22]		4.372	4.372	4.732	1.01	γ
$TiH_{1.75}$	*abcdefg*	−5.115	4.325	4.325	4.558	1.05	γ
		−5.093	4.445	4.445	4.316	0.97	ε
		−5.093	4.402	4.402	4.402	1.00	δ
TiH_2	*abcdefgh*	−5.856	4.319	4.319	4.638	1.07	γ
		−5.844	4.570	4.570	4.218	0.93	ε
	Expt. [4]		4.53	4.53	4.28	0.94	ε
	Calc. [24]		4.486	4.486	4.532	1.01	γ
	Calc. [22]		4.527	4.527	4.199	0.93	ε

for a cubic phase having three independent elastic constants of C_{11}, C_{12}, and C_{44}, the following criteria must be met as the necessary and sufficient conditions for mechanical stability, i.e.

Cubic Criterion 1:

$$C_{11}>0,\ C_{44}>0,\ C_{11}-C_{12}>0,\ (C_{11}+2C_{12})>0 \quad (2a)$$

For a fct phase that has six independent elastic constants of C_{11}, C_{12}, C_{13}, C_{33}, C_{44}, and C_{66}, the

criterion becomes

fct Criterion 1:

$C_{11}>|C_{12}|$, $C_{33}>0$, $C_{44}>0$, $C_{66}>0$, $(C_{11}+C_{33}-2C_{13})>0$, $2(C_{11}+C_{12})+C_{33}+4C_{13}>0$ (2b)

We also notice that there exist other formats of mechanical stability criteria, including

Cubic Criterion 2 [33]:

$C_{11}>0$, $C_{11}^2>C_{12}^2$, $C_{44}>0$ (2c)

fct Criterion 2 [34]:

$C_{11}>|C_{12}|$, $C_{44}>0$, $C_{66}>0$, $C_{33}(C_{11}+C_{12})>2C_{13}^2$ (2d)

fct Criterion 3 [33]:

$C_{11}>0$, $C_{11}^2>C_{12}^2$, $C_{33}(C_{11}+C_{12})>2C_{13}^2$, $C_{11}\cdot C_{33}>C_{13}^2$, $C_{44}>0$, $C_{66}>0$ (2e)

To be prudent, all the above criteria must be simultaneously met to ensure the mechanical stability. All these elastic constants can be explicitly deduced from a series of second-order polynomial relations of total energy versus distortion, by following the procedure of previous first-principles studies [35,36].

Table 2 summarizes all the calculated C_{ij} of TiH_x (x=1−2) with the first and second lowest-energy structures. Obviously, all the C_{ij} values are positive. Thus, the mechanical stability needs only meet $C_{11}>C_{12}$ for cubic phases, and $C_{11}>C_{12}$, $C_{11}+C_{33}>2C_{13}$, $C_{33}(C_{11}+C_{12})>2C_{13}^2$, and $C_{11}\cdot C_{33}>C_{13}^2$ for fct phases (the intersection of fct Criterion 1, 2 and 3), respectively. It can be thus deduced that all the first and second lowest-energy structures as we predicted in Table 1 well meet the above criteria and thus are mechanically stable. That is to say, γ is generally the most energy-favored, mechanically-stable phase for TiH_x (x=1−2) (within the whole hydrogen concentration range of 50%−66.7%). Interestingly, this favorably agrees with the earliest experimental literatures dated back to 1950s [37,38], but obviously conflict with another DFT calculation where γ was predicted as instable and would decompose to α-Ti and δ-TiH_x at low temperatures or transform to δ-TiH_x at higher temperatures within the whole hydrogen range of 50%−66.7% (i.e. x=1−2) [19]. Table 2 also suggests that various different phases, such as TiH-*defg*-ε, $TiH_{1.25}$-*defgh*-γ, $TiH_{1.5}$-*bcefgh*-γ, ε-$TiH_{1.75}$, δ-$TiH_{1.75}$, and ε-TiH_2, can be formed as metastable phases, since they are mechanically stable and have the second-lowest formation energies. Any mechanically instable and/or third-lowest energy structures are arbitrarily excluded.

3.3 Thermodynamics calculations of TiH_x

So far, we have evaluated formation energies and mechanical stabilities of various phases of TiH_x

Table 2 Calculated elastic constants and moduli of TiH_x with first and second lowest-energy structures

Hydride	H-atom configuration	C_{11}	C_{12}	C_{13}	C_{33}	C_{44}	C_{66}	B/GPa	G/GPa	E/GPa
TiH	*adeh*-γ	139.1	136.8	96.9	213.5	59.0	72.3	128.1	48.8	129.8
	defg-ε	170.9	100.6	120.1	118.0	86.4	59.8	122.2	35.4	96.9
	Calc. [23]	143	137	94	225	60	74.2	129.0	51.2	135.7
$TiH_{1.25}$	*bcdf*-γ	134.2	131.1	114.1	184.9	61.9	71.8	130.2	45.4	122.0
	defgh-γ	153.6	116.7	113.8	181.7	89.0	89.0	130.4	52.1	137.8
$TiH_{1.5}$	*bcdfgh*-γ	161.4	123.2	116.5	176.2	73.0	81.1	134.6	54.9	145.1
	bcefgh-γ	150.4	122.5	123.5	167.5	65.4	64.6	133.8	37.4	102.8
	Exp. [39]	–	–	–	–	–	–	125	43	125
	Calc. [23]	188	112	111	189	72.6	81.1	137.0	60.7	158.6
$TiH_{1.75}$	γ	148.8	133.9	128.6	166.1	44.9	45.8	138.4	32.0	89.1
	ε	160.0	130.0	129.3	150.3	49.7	46.7	138.4	29.3	82.0
	δ	150.6	132.1	–	–	41.9	–	138.2	23.1	65.8
TiH_2	γ	151.2	139.3	128.7	179.1	34.5	26.1	141.6	24.7	70.0
	ε	168.8	143.2	123.7	151.2	29.5	40.4	141.1	26.4	74.6
	Calc. [23]	171	155	113	172	12.6	63.8	141.8	26.7	75.3

(x=1−2) at their ground states. To further explore their thermodynamic stabilities under more practical conditions, we calculated the formation energies of TiH_x as a function of T and $p(H_2)$ as

$$\Delta E_f(T,p)=\mu_{TiH_x}(T,p)-\mu_{Ti}(T,p)-\frac{x}{2}\mu_{H_2}(T,p) \quad (3)$$

μ_{H_2} is the chemical potential of gaseous H_2 molecule and can be further expressed as [40]

$$\mu_{H_2}(T,p)=\mu^0_{H_2}(T)+k_BT\ln\frac{p(H_2)}{p^0(H_2)}$$
$$=\mu^0_{H_2}(0\ K)+\Delta H_{H_2}(T)-TS_{H_2}(T)+k_BT\ln p(H_2) \quad (4)$$

where $p^0(H_2)=10^5$ Pa, and k_B is the Boltzmann constant. Note that the free energy of a solid bulk phase is always much less sensitive to T and $p(H_2)$ as compared to a gaseous molecule. Also, a large cancellation occurs between the first two energy terms of bulk phases μ_{TiH_x} and μ_{Ti} in Eq. (3). Thus, the temperature and pressure dependence of ΔE_f dominantly arises from the gaseous H_2 molecule. With this approximation, we can rewrite Eq. (3) to be

$$\Delta E_f(T,p)=\mu^0_{TiH_x}(0\ K)-\mu^0_{Ti}(0\ K)-\frac{x}{2}[\mu^0_{H_2}(0\ K)+$$
$$\Delta H_{H_2}(T)-T\Delta S_{H_2}(T)+k_BT\ln p(H_2)] \quad (5)$$

Here, $\Delta H_{H_2}(T)$ and $\Delta S_{H_2}(T)$ can be referred to the experimental values as tabulated in JANAF tables [41]. Obviously, the formation energy of TiH_x is no longer a constant value but varies with the environmental conditions (T and $p(H_2)$). The upper limit of $p(H_2)$ is set as $p(H_2)\leq p^0(H_2)$, by requiring no net hydrogen release from the hydride under the thermodynamic equilibrium.

Figures 2 and 3 compare the calculated formation energies for various stable and metastable phases of TiH_x, respectively. Specifically, Fig. 2 is plotted for all the stable γ phases of TiH_x (x=1, 1.25, 1.5, 1.75 and 2), each with the lowest energy H atom configuration of TiH-*adeh*-γ, $TiH_{1.25}$-*bcdfg*-γ, $TiH_{1.5}$-*bcdfgh*-γ, $TiH_{1.75}$-γ and TiH_2-γ, respectively. Figure 3 is plotted for all the metastable phases including TiH-*defg*-ε, $TiH_{1.25}$-*defgh*-γ, $TiH_{1.5}$-

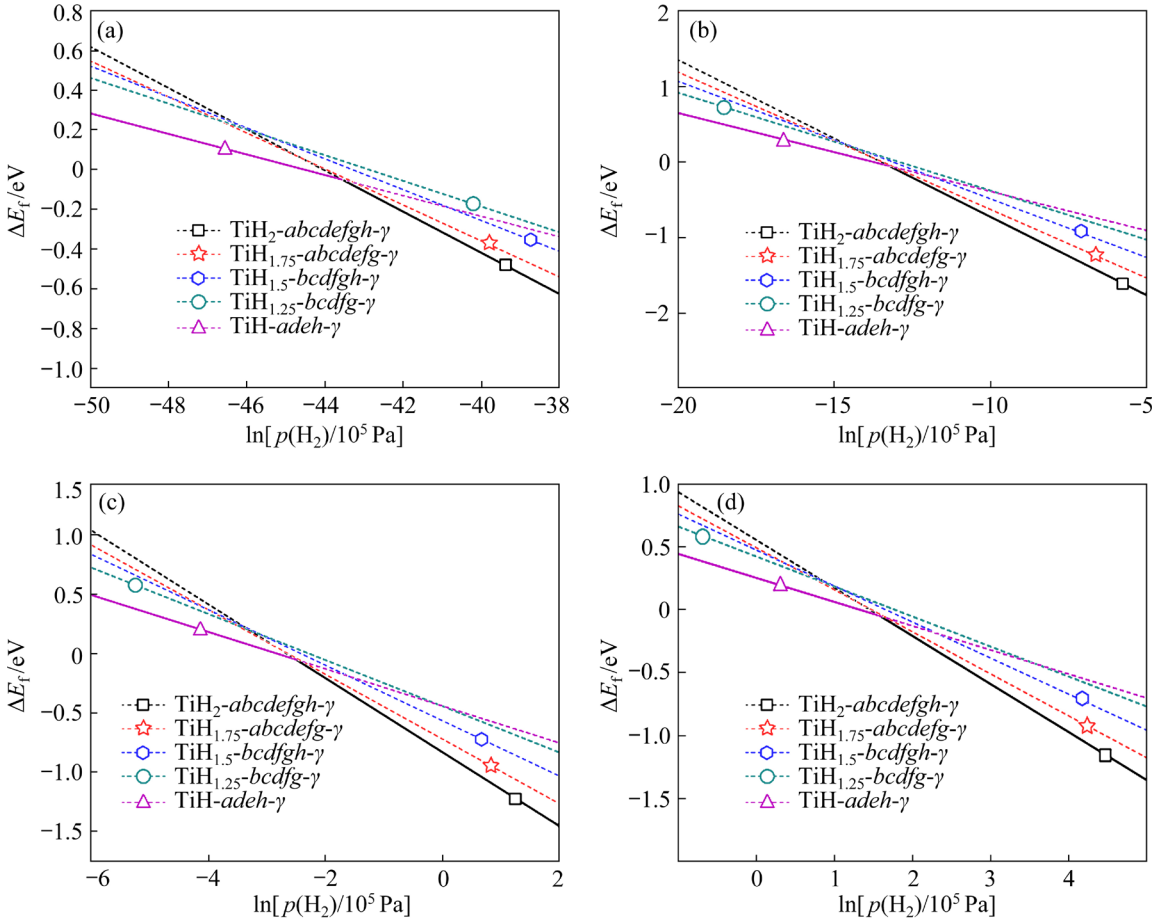

Fig. 2 Calculated formation energies of various stable TiH_x (x=1−2) phases as function of $p(H_2)$ at different temperatures: (a) 300 K; (b) 600 K; (c) 900 K; (d) 1100 K

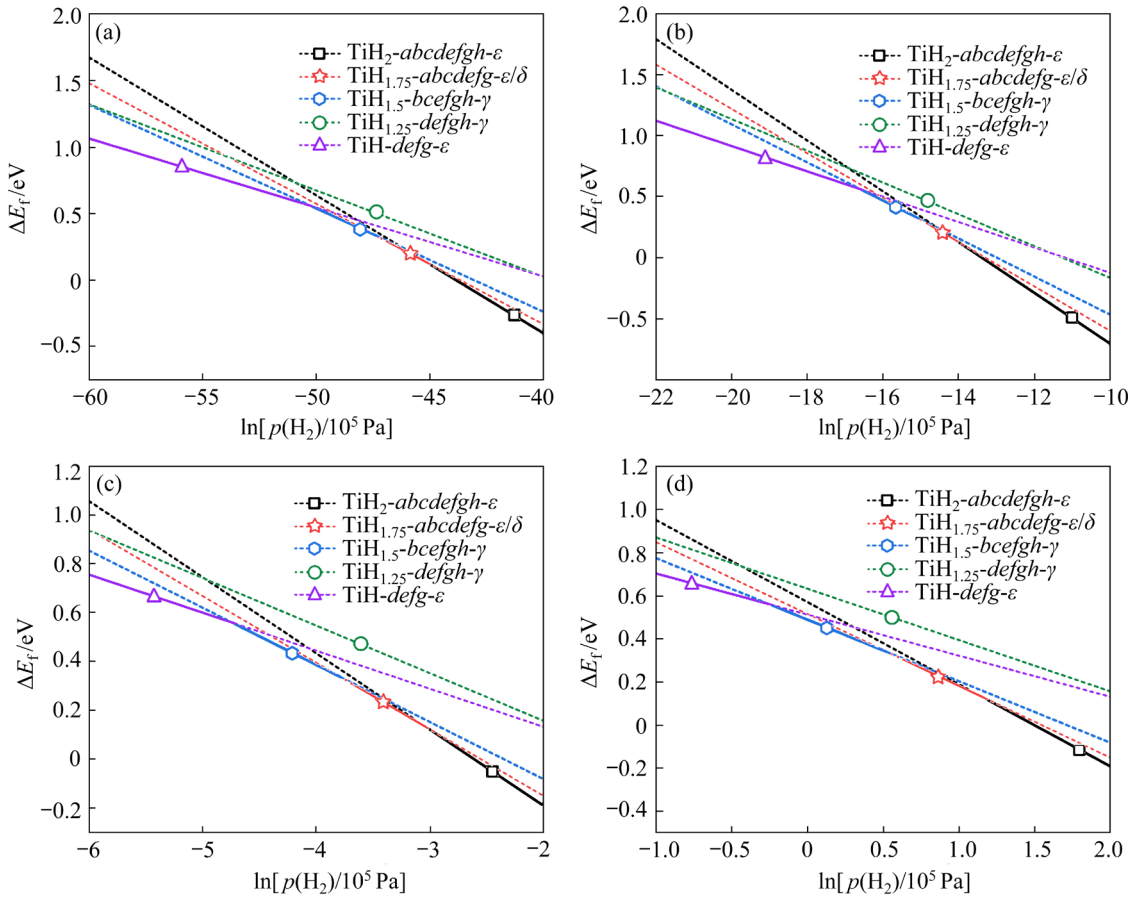

Fig. 3 Calculated formation energies of various metastable TiH_x (x=1−2) phases as function of $p(H_2)$ at different temperatures: (a) 300 K; (b) 600 K; (c) 900 K; (d) 1100 K

bcefgh-γ, $TiH_{1.75}$-ε, $TiH_{1.75}$-δ and TiH_2-ε. Among them, $TiH_{1.75}$-ε has the same formation energy and the same H-atom configuration as $TiH_{1.75}$-δ, and both would be always equally favored with the same stabilities at any given thermodynamic condition. It is manifested in Figs. 2 and 3 that the formation energy of a TiH_x phase always decreases with the increasing $p(H_2)$ at any temperature. The slope has been suggested by Eq. (5) to be inversely proportional to the H content of x. Under a given T and $p(H_2)$, the lowest formation energy predicts the most stable structure. Thus, the intersection of any two arbitrary lines in Figs. 2 and 3 predicts the critical $p(H_2)$ value for initiating a phase transition, and tracking the lowest critical $p(H_2)$ values at different temperatures would enable us to construct the stable and metastable phase stability diagrams of the Ti−H system in Fig. 4.

Figures 2 and 3 were just plotted for four different temperatures. To construct Fig. 4, the critical $p(H_2)$ values were calculated for fourteen different temperatures within the range of 300−1000 °C, each with a temperature interval of 50 °C, and smoothed curves were plotted. It has been revealed in Fig. 2 that, over the entire range of T and $p(H_2)$ being considered, γ-TiH and γ-TiH_2 phases take the lead in having the lowest formation energy, while all other stable TiH_x phases have relatively higher formation energies. Thus, the only possible phase transition occurs between γ-TiH and γ-TiH_2, dividing the stable phase stability diagram in Fig. 4(a) into two regions. γ-TiH dominates in the upper region with relatively higher T and/or lower $p(H_2)$, while γ-TiH_2 dominates in the lower region with relatively lower T and/or higher $p(H_2)$. According to Table 1, the phase transition from γ-TiH to γ-TiH_2 would be accompanied by a volume expansion of ~8% and a deduction of c/a from 1.1 to 1.07. It is also reminded that Fig. 4(a) can only predict the thermodynamic stabilities of TiH_x phases under the equilibrium conditions. Some lowest-energy TiH_x phases, such as γ-$TiH_{1.25-1.75}$ predicted in Table 1, cannot be stable at any given T and $p(H_2)$ but have a thermodynamic tendency to

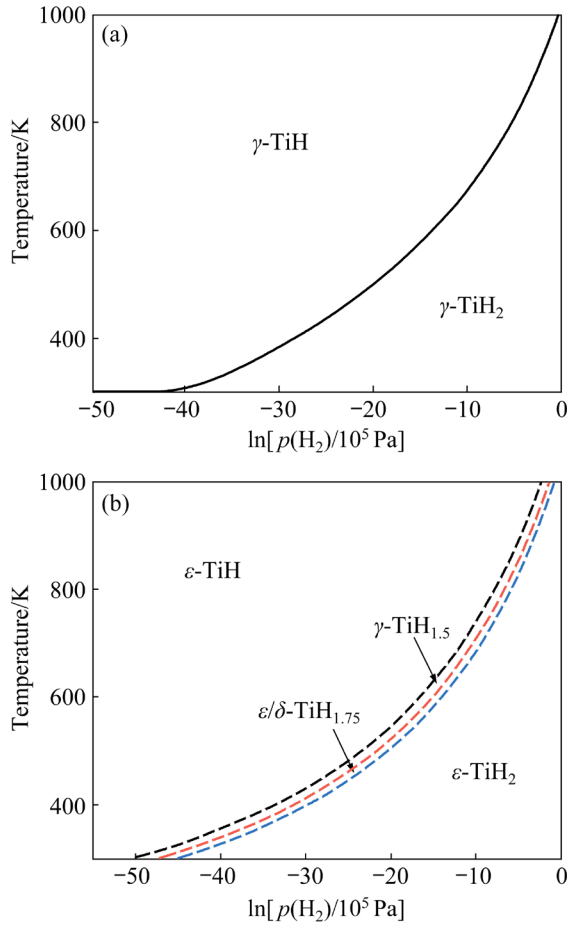

Fig. 4 Calculated stable (a) and metastable (b) phase stability diagrams of TiH_x (x=1−2)

continuously adsorb (or release) H until reaching the equilibrium phase γ-TiH_2 (or γ-TiH), depending on the real-time conditions of T and $p(H_2)$. The calculated metastable phase stability diagram is plotted for a comparison in Fig. 4(b). Again, a metastable phase is defined as a mechanically stable structure with the second-lowest energy at a given H content of x. ε-TiH and ε-TiH_2 take the lead as metastable phases in dominating the most range of T and $p(H_2)$, making an essential two-region diagram. γ-$TiH_{1.5}$ and ε-$TiH_{1.75}$ and δ-$TiH_{1.75}$ locate between the two regions, which also present as metastable phases within certain extremely narrow ranges of T and $p(H_2)$.

Obviously, the stabilities of TiH_x (x=1−2) sensitively depend on the thermodynamic conditions of T and $p(H_2)$. The experimental characterizations of TiH_x in the published literatures have involved many disputes. This fact can be strongly related to our findings that various TiH_x phases have very comparable formation energies and mechanical stabilities under a given T and $p(H_2)$, and thus they possibly co-present as stable or metastable phases in experiments. Moreover, H atoms diffuse fairly fast among different hydride phases, which brings increased challenges to experimental characterization. It is highly suggested that the stable and metastable phase stability diagrams in Fig. 4 shall be combined in uses, for predicting TiH_x phases and their relative stabilities under a given thermodynamic condition.

4 Conclusions

(1) Energetics calculations suggested that TiH and $TiH_{1.25}$ have double energy minima, corresponding to the common phase fct-γ (c/a>1) and an orthorhombic phase ($a\neq b\neq c$) that has never been reported in the literatures. $TiH_{1.5}$ is a γ phase but may have various different H atom configurations with very similar formation energies. $TiH_{1.75}$ is most likely to be a γ phase, immediately followed by other two phases of δ and ε with the same formation energy. TiH_2 is almost equally likely to be a γ or ε phase.

(2) The elastic constant tensor calculations suggested that all the first and second-lowest energy structures of TiH_x phases (x=1, 1.25, 1.5, 1.75, and 2) are mechanically stable. These second-lowest energy structures can be regarded as metastable phases. The formation energies of TiH_x phases, whether stable or metastable, always decrease with the increasing hydrogen partial pressure, $p(H_2)$.

(3) The constructed phase stability diagram predicted only two stable phases of γ-TiH and γ-TiH_2. γ-TiH dominates at higher T and/or lower $p(H_2)$, while γ-TiH_2 dominates at lower T and/or higher $p(H_2)$. The metastable phase stability diagram predicted two major metastable phases of ε-TiH and ε-TiH_2. Other three metastable phases γ-$TiH_{1.5}$ and ε-$TiH_{1.75}$ and δ-$TiH_{1.75}$ may exist in their narrow transition regions. Especially, metastable ε-$TiH_{1.75}$ is always equally preferred as metastable δ-$TiH_{1.75}$. The combined use of the stable and metastable phase stability diagrams is highly encouraged for predicting the environment-sensitive phase structures of TiH_x (x=1−2) during the hydrogenation practice of titanium.

Acknowledgments

This work was financially supported by the

National MCF Energy R&D Program of China (No. 2018YFE0306100), and the National Natural Science Foundation of China (No. 51971249). The computational resources at Hefei Advanced Computing Center and the High-Performance Computing Center of Central South University are also highly appreciated.

References

[1] WILLIAM M M. CHAPTER 8-titanium hydrides [M]. USA: Academic Press, 1968: 336−383.

[2] WEAVER B, WALL W R. DOE handbook: Tritium handling and safe storage [M]. Washington D C: United States Department of Energy, 1999: 1129−1199.

[3] ROKHMANENKOVA A, YANILKIN A. Simulation of hydrogen thermal desorption and stability titanium hydrides TiH [J]. International Journal of Hydrogen Energy, 2019, 44(55): 29132−29139.

[4] MANCHESTER F D, SAN-MARTIN A. The H−Ti (hydrogen−titanium) system [J]. Bulletin of Alloy Phase Diagrams, 1987, 8(1): 30−42.

[5] ZUZEK E, ABRIATA J P, SAN-MARTIN A, MANCHESTER F D. The H−Zr (hydrogen−zirconium) system [J]. Bulletin of Alloy Phase Diagrams, 1990, 11(4): 385−395.

[6] UKITA S, OHTANI H, HASEBE M. Thermodynamic analysis of the Ti−H and Zr−H binary phase diagrams [J]. Journal of the Japan Institute of Metals, 2007, 71(9): 721−729.

[7] GORING R, LUKAS R, BOHMHAMMEL K. Multipulse NMR investigation of band structure in titanium hydride: Proton Knight shift and spin-lattice relaxation [J]. Journal of Physics C, 1981, 14(36): 5675−5687.

[8] FRISCH R C, FORMAN R A. Nuclear magnetic resonance of Ti in Ti−H systems [J]. Journal of Chemical Physics, 1968, 48: 5187−5190.

[9] EHRENFREUND E, WEGER M, KORN C, ZAMIR D. Nuclear spin relaxation times of protons in titanium-hydride alloys [J]. Journal of Chemical Physics, 1969, 50: 1907−1908.

[10] KORN C, GOREN S D. Model-independent NMR approach in determining hydrogen diffusion in titanium hydride [J]. Physical Review B, 1986, 33(1): 64−67.

[11] KORN C. Nuclear-magnetic-resonance study of the electronic structure of the Ti−H system [J]. Physical Review B, 1978, 17(4): 1707−1720.

[12] TAO S X, NOTTEN P H L, van SANTEN R A, JANSEN A P J. Density functional theory studies of the hydrogenation properties of Mg and Ti [J]. Physical Review B, 2009, 79(14): 144121.

[13] WANG Xin-quan, WANG Jian-tao. Structural stability and hydrogen diffusion in TiH_x alloys [J]. Solid State Communications, 2010, 150(35/36): 1715−1718.

[14] NUMAKURA H, KOIWA M, ASANO H, MURATA H, IZUMI F. X-ray diffraction study on the formation of γ titanium hydride [J]. Scripta Metallurgica, 1986, 20(2): 213−216.

[15] KOLESNIKOV A I, BALAGUROV A M, BASHKIN I O, FEDOTOV V K, MALYSHEV V Y, MIRONOVA G M, PONYATOVSKY E G. A real-time neutron diffraction study of phase transitions in the Ti−D system after high-pressure treatment [J]. Journal of Physics: Condensed Matter, 1993, 5(29): 5045−5058.

[16] WANG Kun, KONG Xiang-cheng, DU Jun-lin, LI Chong-he, LI Zhi-lin, WU Zhu. Thermodynamic description of the Ti−H system [J]. Calphad, 2010, 34(3): 317−323.

[17] OKAMOTO H. H−Ti (hydrogen−titanium) [J]. Journal of Phase Equilibria and Diffusion, 2011, 32(2): 174−175.

[18] NUMAKURA H, KOIWA M. Hydride precipitation in titanium [J]. Acta Metallurgica, 1984, 32(10): 1799−1807.

[19] XU Qing-chuan, van der VEN A. First-principles investigation of metal-hydride phase stability: The Ti−H system [J]. Physical Review B, 2007, 76(6): 064207.

[20] LIANG Chao-ping, GONG Hao-ran. Fundamental mechanism of tetragonal transitions in titanium hydride [J]. Materials Letters, 2014, 115: 252−255.

[21] POLETAEV D O, AKSYONOV D A, VO D D, LIPNITSKII A G. Hydrogen solubility in hcp titanium with the account of vacancy complexes and hydrides: A DFT study [J]. Computational Materials Science, 2016, 114: 199−208.

[22] OLSSON P A T, BLOMQVIST J, BJERKÉN C, MASSIH A R. Ab initio thermodynamics investigation of titanium hydrides [J]. Computational Materials Science, 2015, 97: 263−275.

[23] LIANG Chao-ping, GONG Hao-ran. Atomic structure, mechanical quality, and thermodynamic property of TiH_x phases [J]. Journal of Applied Physics, 2013, 114(4): 043510.

[24] MIWA K, FUKUMOTO A. First-principles study on 3d transition-metal dihydrides [J]. Physical Review B, 2002, 65(15): 155114.

[25] DING R, JONES I P. In situ hydride formation in titanium during focused ion milling [J]. Journal of Electron Microscopy, 2010, 60(1): 1−9.

[26] KRESSE G, FURTHMÜLLER J. Efficient iterative schemes for ab initio total-energy calculations using a plane−wave basis set [J]. Physical Review B, 1996, 54(16): 11169−11186.

[27] KRESSE G, JOUBERT D. From ultrasoft pseudopotentials to the projector augmented-wave method [J]. Physical Review B, 1998, 59(3): 1758−1775.

[28] BLÖCHL P E. Projector agmented-wave method [J]. Physical Review B, 1994, 50(24): 17953−17979.

[29] PERDEW J P, BURKE K, ERNZERHOF M. Generalized gradient approximation made simple [J]. Physical Review Letters, 1996, 77(18): 3865−3868.

[30] KHODA-BAKHSH R, ROSS D K. Determination of the hydrogen site occupation in the α phase of zirconium hydride and in the α and β phases of titanium hydride by inelastic neutron scattering [J]. Journal of Physics F: Metal Physics, 1982, 12(1): 15−24.

[31] ZHANG Peng, WANG Ban-tian, HE Chao-hui, ZHANG Ping. First-principles study of ground state properties of ZrH_2 [J]. Computational Materials Science, 2011, 50(12): 3297−3302.

[32] NYE J F. Physical properties of crystals [M]. USA: Oxford

University Press, 1957: 13−16.
[33] SADD M H. Elasticity theory, applications, and numerics [M]. USA: Elsevier Incorporation, 2005: 291−292.
[34] MOUHAT F, COUDERT F X. Necessary and sufficient elastic stability conditions in various crystal systems [J]. Physical Review B, 2014, 90(22): 224104.
[35] JIANG Yong, SMITH J R, ODETTE G R. Prediction of structural, electronic and elastic properties of $Y_2Ti_2O_7$ and Y_2TiO_5 [J]. Acta Materialia, 2010, 58(5): 1536−1543.
[36] DOBSON P J. Physical properties of crystals−Their representation by tensors and matrices [J]. Physics Bulletin, 1985, 36(12): 506−506.
[37] MCQUILLAN A D. An experimental and thermodynamic investigation of the hydrogen-titanium system [J]. The Royal Society, 1950, 204(1078): 309−322.
[38] HAGG R M, SHIPKO F J. The titanium-hydrogen system [J]. American Chemical Society, 1956, 78(20): 5155−5159.
[39] SETOYAMA D, MATSUNAGA J, MUTA H, UNO M, YAMANAKA S. Mechanical properties of titanium hydride [J]. Journal of Alloys and Compounds, 2004, 381(1/2): 215−220.
[40] JIANG Yong, ADAMS J B, SCHILFGAARDE M V. Density-functional calculation of CeO_2 surfaces and prediction of effects of oxygen partial pressure and temperature on stabilities [J]. The Journal of Chemical Physics, 2005, 123: 64701.
[41] ROSSINI F D. JANAF thermochemical tables [J]. The Journal of Chemical Thermodynamics, 1972, 4(3): 509−510.

依赖环境的氢化钛相稳定性：第一性原理预测

沈春雷[1]，刘 艺[2]，宫裕祥[2]，刘正卿[2]，江 勇[2,3]，许灿辉[1]，周晓松[1]，龙兴贵[1]

1. 中国工程物理研究院 核物理与化学研究所，绵阳 621900；
2. 中南大学 材料科学与工程学院，长沙 410083；
3. 中南大学 粉末冶金国家重点实验室，长沙 410083

摘 要：在充分考虑所有可能的 H 原子构型的条件下，构建各种 TiH_x(x=1−2)相结构，并基于第一性原理能量学，计算评估各相的形成能力及其力学和热力学稳定性，进而构建稳定和亚稳 TiH_x 的相稳定性图。结果显示，很多稳定和亚稳 TiH_x 相具有非常接近的形成能，可能同时共存。这些相的相对稳定性强烈依赖于环境温度(T)和氢分压($p(H_2)$)。在整个感兴趣的 T 和 $p(H_2)$范围内，只可能存在 γ-TiH 和 γ-TiH_2 2 种稳定相，以及 ε-TiH、γ-$TiH_{1.5}$、ε-$TiH_{1.75}$、δ-$TiH_{1.75}$ 和 ε-TiH_2 5 种亚稳相。这些亚稳相均满足力学稳定性，且在热力学上具有不断吸收或释放 H，向平衡相 γ-TiH_2 或 γ-TiH 发生转化的趋势。

关键词：氢化钛；相稳定性；亚稳相；第一性原理

(Edited by Bing YANG)